Environmental Science Nano

Accepted Manuscript

This article can be cited before page numbers have been issued, to do this please use: J. Gigault, B. Pedrono, B. Maxit and A. ter Halle, *Environ. Sci.: Nano*, 2016, DOI: 10.1039/C6EN00008H.

ROYAL SOCIETY OF CHEMISTRY

rsc.li/es-nano

View Article Online
DOI: 10.1039/C6EN00008H

Nano- Impact statement.

This work is based on our hypothesis that something is missing in the study of marine anthropogenic litters after our expedition (Expedition 7th Continent). Based on our hypothesis, we developed for the first time a new solar reactor equipped with an in-situ dynamic light scattering detector to investigate the possibility of the formation of nano-plastics from millimeter scale plastics. With this system, complemented with electronic microscopy observations, we present undeniable evidence of nano-plastic occurrence due to the solar light degradation of marine micro-plastics under controlled and environmentally representative conditions. These unprecedented results show the new potential hazards of plastic waste at the nanoscale, which had not been taken into account previously.

View Article Online
DOI: 10.1039/C6EN00008H

Environmental Science: Nano

COMMUNICATION

Marine plastic litters: the unanalyzed nano-fraction

Julien Gigault[a], Boris Pedrono[b], Benoît Maxit[b], and Alexandra Ter Halle[c]

Received 00th January 20xx,
Accepted 00th January 20xx

DOI: 10.1039/x0xx00000x

www.rsc.org/

In this work, we present for the first time undeniable evidence of nano-plastic occurrence due to solar light degradation of marine micro-plastics under controlled and environmentally representative conditions. As observed during our recent expedition (Expedition 7th Continent), plastic pollution will be one of the most challenging ecological threats for the next generation. Up to now, all studies have focused on the environmental and the economic impact of millimeter scale plastics. These plastics can be visualized, collected and studied. We are not aware of any studies reporting the possibilities of nano-plastics in marine water. Here, we developed for the first time a new solar reactor equipped with a nanoparticle detector to investigate the possibility of the formation of nano-plastics from millimeter scale plastics. With this system, correlated with electronic microscopy observations, we identified for the first time the presence of plastics at the nanoscale in water due to UV degradation. Based on our observations large fractal nano-plastic particles (i.e., >100 nm) are produced by UV light after the initial formation of the smallest nano-plastic particles (i.e., <100 nm). These new results show potential hazards of plastic waste at the nanoscale, which had not been taken into account previously.

We are not aware of any studies reporting the occurrence of nano-plastics in marine water, and only millimeter scale materials are referenced [1,2]. This lack of evidence is due to (i) the dilution of nano-plastics on the ocean surface and (ii) the lack of appropriate methodologies for characterizing nanoscale materials in the environment [3,4]. In a recent review, some authors reported that there is a doubt that nanoscale particles could be produced by the weathering of plastic debris and indicated a lack of analytical methods for quantifying these particles [3,5,6]. Cozar et al. identified a deficiency of marine plastic particles at the lower end of the size distribution (<1 mm) in the abundance diagram and argued that fast nano-fragmentation from millimeter scale debris might be a plausible explanation for this deficiency [7]. Due to the technical limitations, others authors clearly indicate that plastic litters at the nanoscale are omitted compare to sub-1mm[8]. Indeed, it is easily acceptable to imagine the accelerated physical and chemical degradation of plastics from the millimeter scale to the nanometer scale, especially considering the extreme conditions (temperature, salinity, bioactivity, and UV light) of ocean systems. Here, we present for the first time undeniable evidence of nano-plastic occurrence due to solar light degradation of marine micro-plastics under controlled and environmentally representative conditions.

As described in the main text, we first developed a homemade photo-reactor to simulate solar light for degrading plastics with in-situ measurements of the particle size by a dynamic light scattering probe (see Methods section). The irradiated plastic was composed of micro-plastic fragments collected from the North Atlantic gyre during the sea campaign Expedition 7th Continent [9]. The micro-plastics are millimeters wide, mostly between 1 and 2 mm. The composition of the micro-plastics is determined by infrared spectroscopy and is 90% polyethylene and 10% polypropylene (see supplemental information, S.4.). The micro-plastics collected from the gyre presented an advanced state of weather-

[a] Environnements et Paléo-Environnements Océaniques et Continentaux, French National Center of Scientific Research (CNRS, UMR 5805), 351 Cours de la Libération, 33405 Talence Cedex. *Email: julien.gigault@u-bordeaux.fr.
[b] Cordouan Technologies, 11 Avenue de Canteranne, 33600 Pessac.
[c] Laboratoire des Interactions Moléculaires et réactivité Chimique et Photochimique (IMRCP), UMR CNRS 5623, Université Paul Sabatier-UPS, Bâtiment 2R1, 3ème étage, 118, route de Narbonne, 31062 Toulouse Cedex 09, France. Email : ter-halle@chimie.ups-tlse.fr.

Electronic Supplementary Information (ESI) available: [details of any supplementary information available should be included here]. See DOI: 10.1039/x0xx00000x

View Article Online
DOI: 10.1039/C6EN00008H

ing; for example, the carbonyl index was typically between 0.2 and 1.6.

These microplastics are floating at the surface of ultra-pure water within hermetic quartz cell and endure UV irradiation while an intermediary volume is probed continuously with a customized in-situ Dynamic Light Scattering (DLS) device. This unique technology, dedicated to give size distributions of particles without sampling and manipulation, allowed us to demonstrate the evidence of colloidal materials. Two parameters are monitored regularly according to the UV exposure time:

- The photon count rate corresponding to the average scattered light signal (as illustrated on Figure 1a); the scattered intensity is directly related to the number and the size of scattering objects within the probed volume
- The autocorrelation function (ACF) of the scattered light (Figure 1b); negative exponential trends of the ACF are the signature of diffusion process of nano-objets.

Indeed, when colloidal materials are studied in DLS, the diffusion coefficient *D* is proportional to the decay rate of the ACF when particles are enduring Brownian motion. In extension, according to the Stokes-Einstein equation, D is also inversely proportional to the nano-object size. As a consequence, the higher the decay rate, the smaller the particle size. Regularization algorithms are currently used to fit this ACF as a distribution of decay rates then a distribution of particles sizes.

The reference measurement performed before applying UV irradiation (t=0 min) corresponds to the one expected with ultra-pure water only (insignificant count-rate and no ACF relaxation - blue curve in Fig.1b). Standard reference materials were analyzed respecting the same order of dilution of the nano-plastics in order to demonstrate that the instrument is operating properly (see SI, Fig. S2). Then we observed a continuous increase of the count rate over time, which confirm the presence of more scattering species and/or the detection of larger size objects. In the same time we noticed important changes in ACF according to the UV exposure time. 23 hours after we initiated the UV exposition, negative exponential decay begins to be clearly observed (red curve), which indicates the presence of small colloidal materials. Yet, the signal weakness and the predominant noise still lead to unreliable size analysis. Then, from 23 hours to 75 hours (in green), the process continues with a better ACF curve resolution with two noticeable decay rates (fast and slow). Size evaluation indicates two distinguishable polydispersed populations (<400nm and beyond 2 µm). At this time, size analysis is then approximate since particles are too diluted. The ACF shift became quite stable from 75 hours to 128 hours (in black). We observed a transition from the ACFs similar to the first time intervals (small particles) to the second decay rate at longer times indicating the presence of larger particles. Size evaluation confirms the same population under 400nm but a shift of the second size population forward 10 µm. Between 128 and 358 hours, slowest decay rates become predominant hiding the fastest ones. That reveals the presence of increasing concentration of micrometric objects - Size analysis is then inappropriate since particles are too big and no more in Brownian motion. That also explains the increase in count rate. Visually, when comparing the irradiated solution at t=0 with the period after 358 hours we observed many light spots (scattered light) under the laser beam, which are characteristic of a particle population.

Based on the in-situ DLS analysis, two major hypotheses can be made about nano-particle formation during photo-degradation:

(i) Small nanoparticles are first produced, and then they rearrange themselves to form larger aggregates. The bimodal size distribution is generally characterized by an autocorrelation function representing different decay rates, as observed in figure 1b.

(ii) Small nanoparticles are first produced, which generates more and more defects in the initial millimeter sized plastic particle. The increase in defects induces the degradation of larger particles. Such degradation will produce randomly shaped particles. Non-spherical particles possess diffusion properties that are different from ideal spheres, and *D* is the sum of the complex motions induced by shape (rotation, translation, etc.) and is also characterized by an autocorrelation function with different decay rates.

Nevertheless, the water volume was overvalued compared to the final degraded product i.e. the colloidal concentration is too low to create strong scattering signal and obtain a highly reliable polymodal and polydispersed size distribution of the nano-plastics. Due to the low concentration and a lack of appropriate methodology for characterizing and quantifying colloidal materials at trace concentrations, it was difficult to accurately characterize and quantify the nano-plastics. To confirm the effective trends, TEM imaging was performed after concentrating the sample. A concentration method was developed based on ultrafiltration. The initial concentration and volume were decreased by a ratio of 50 by fractionating sizes over 10 kDa. The concentrating 1 mL

View Article Online
DOI: 10.1039/C6EN00008H

solution was then prepared for TEM analysis (see Methods section for details of sample preparation). Figure 2 presents the TEM images of the concentrating solution at different magnification levels (200 nm and 500 nm scale bars). These two pictures are representative of the entire sample (selection from sets of multiple TEM pictures of several grids). The representativeness of the sample is characterized by (i) the size distribution and (ii) the inhomogeneous shape of the particles characterized. On the pictures with a scale bar of 500 nm, we clearly identified heterogeneity in size and shape. The right figure shows a considerable quantity of smaller particles <100 nm with a few large particles over 100 nm. The nanoparticles were characterized by very high polydispersity, ranging from a few nanometers (i.e., 3-4 nm) up to 500 nm and a maximum population located at 230 nm. This result is clearly in accordance with DLS results.

While the smallest particles (i.e., < 50 nm) look spherical, the larger ones seem to be randomly shaped. Stars and others fractal particles are visible. Such observations confirm the first hypothesis made from the in-situ DLS results. These pictures present undeniable proof of the presence of plastics in the water at the nanoscale after UV degradation. The dark film that appears on the pictures is characteristic of the high electron density molecules present in the solution. Generally, these molecules are salt, ions and other small molecules attached, adsorbed or absorbed in the polymeric matrices. These species are essentially located around the nano-plastics that induced these dark and blurry aspects.

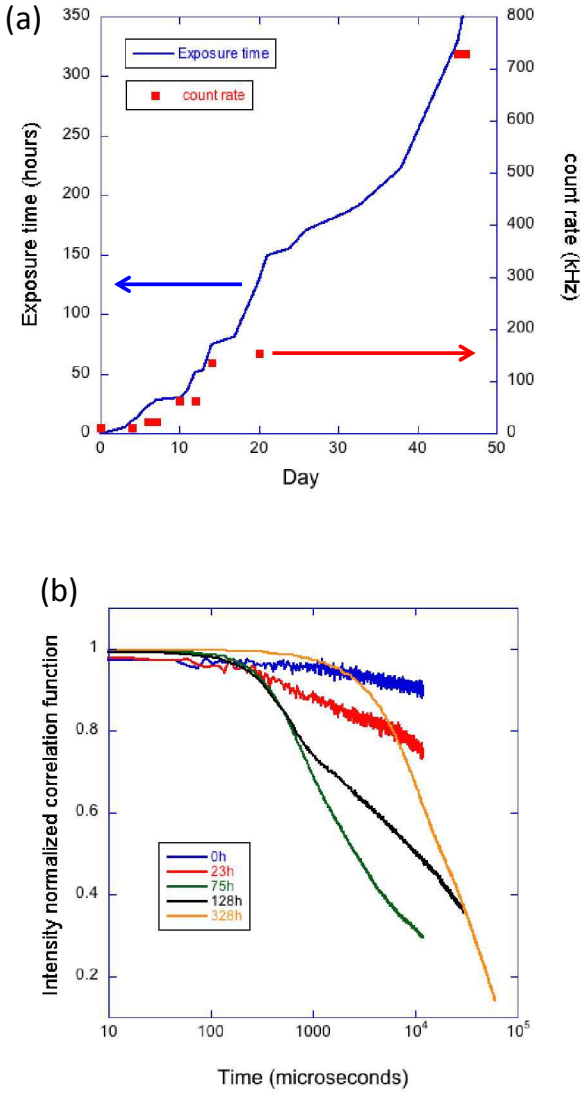

Figure 1: (a) UV exposition time according to the day of running experiments (The UV exposition time corresponds to the time where the UV lamp was turned on); (b) auto-correlation function measured by the DLS probe according to the UV exposition time.

View Article Online
DOI: 10.1039/C6EN00008H

Environmental Science: Nano

COMMUNICATION

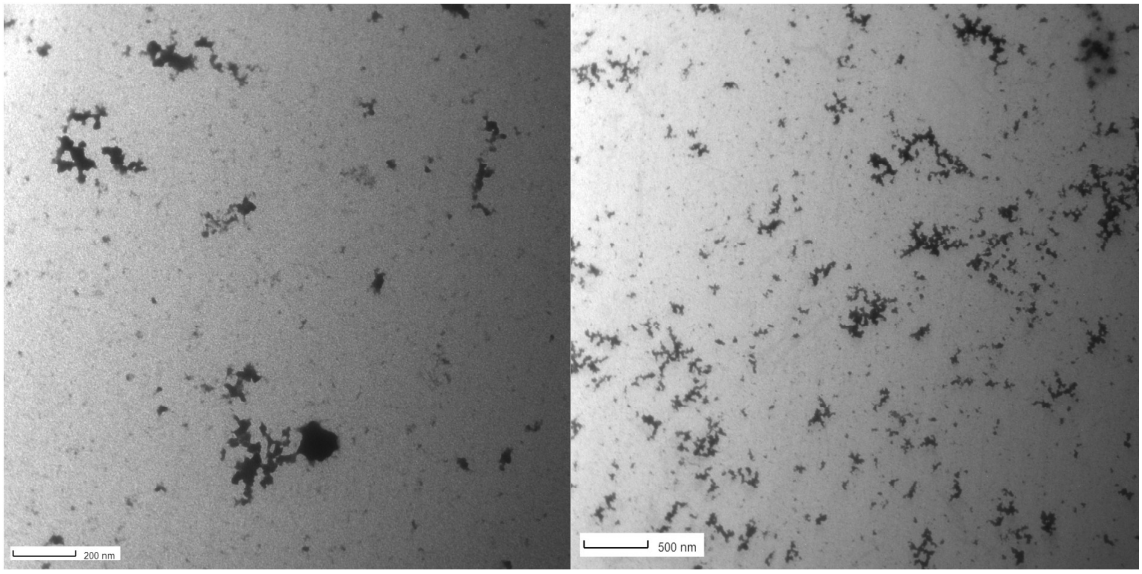

Figure 2: TEM image of nano-plastics; the images scales are 200 nm and 500 nm for the left and right pictures respectively.

The main cause of plastic degradation is photo-oxidation by the combined actions of UV light and oxygen [10]. Contrary to mechanical aging, this leads to chemical changes in the polymeric chains. Photochemical degradation occurs mainly on the film surface. The oxidation progress inside the polymer decreases with depth because it is dependent on the oxygen absorption capacity (limiting factor) of the material [11,12]. The degradation phenomena involved during photo-degradation are common mainly involve chain scissions and cross-linking reactions [13–16]. Plastics are subjected to chemical reactions when exposed to the outdoors. In fact, the absence of any type of stabilizer makes it very sensitive to UV light due to the number of structural defects that are acquired either during polymerization or during processing [17–19]. In addition to direct plastic photo-degradation, indirect photo-degradation is also worth considering (induced by many natural species including colloidal or dissolved organic matter)[20]. A combination of photo and bio-degradation is also conceivable[21].

The aging of polyethylene induces many changes in chemical structure [22,23] and morphology. The surfaces of marine plastic debris are rough and uneven [24]. The plastic becomes crumbly. The advanced state of oxidation of marine micro-plastics makes these materials highly sensitive to photo-degradation due to structural defects, unsaturation and the formation of hydro-peroxides that are highly photo-reactive.

Conclusions

To conclude, our work has identified for the first time the presence of plastics at the nano-scale in water due to UV degradation. These results suggest an increase in the potential hazards of plastic waste by considering the nano-scale, which have not been taken into account yet. It is difficult and challenging to determine the mechanisms of nano-plastic formation. Nevertheless, based on our observations and knowledge of the process of plastic degradation by UV light, the present hypothesis seems to be the most plausible: large fractal particles are produced by UV light after the initial formation of the smallest nanoparticles, which creates favorable defects in the material. In our case, the formation of small nano-

View Article Online
DOI: 10.1039/C6EN00008H

plastics (i.e., <100 nm) was favored by the fact that the micro-plastics were already in an advanced state of oxidation (they had been previously degraded in natural systems before exposure). More work is currently engaged to investigate the environmental fate and behavior of nano-plastics, but also on the compositional analysis of the particles (e.g., A4F-ICPMS, SEM/STEM with EDX analysis) in order to determine the possible colloidal and dissolved species attached to these nano-plastics

Methods

Plastics sampling and preparation.

Micro-plastics were collected in the North Atlantic accumulation zone on the 21st of May, 2014. We undertook net towing for 60 minutes in the location (N25.09727 and W 58.82853) while the ship was travelling at a speed of 2 to 3 knots. These tow nets sampled the air-sea interface. The seawater was filtered at a depth of 0-30 cm using a Manta net with a mouth of 50 cm x 30 cm and a mesh of 300 µm. After the net tow, the collected material was transferred to a container filled with seawater. The micro-plastic particles were extracted with a tweezer, rinsed and stored in a glass vial at + 5°C for further analysis or experiment.

Infrared spectroscopy.

The infrared spectrum was recorded by attenuated total reflectance (ATR) using a diamond ATR crystal in a ThermoNicolet Nexus apparatus. All images were taken at a nominal spectral resolution of 4 cm^{-1} using 16 scans. The recorded data were corrected to obtain transmission-like spectra using the ATR Thermo correction (assuming the refractive index of the sample was 1.5) (see ATR-FTIR spectrum in SI, Fig S3). The carbonyl index (I_{CO}) is defined as the absorbance of carbonyl moieties relative to the absorbance of the reference peaks (methylene moieties). The carbonyl absorption bands were considered to be in the region of 1760-1690 cm^{-1}; and the methylene absorption band was taken to be in the region of 1490-1420 cm^{-1} (methylene scissoring peak).

UV-degradation with in-situ DLS detection.

The photo-reactor is composed of two parts and the solution is placed at the interface in a quartz cell. The bottom part is the UV lamp (HTC Supratec 400-241, Osram GmbH) covering the solar wavelength (280 to 400 nm, UVB to UVA). A total UV energy of 1000 W m^{-2} according to the wavelength was delivered to the solution. The temperature was kept constant at 293 K in the bottom part by air-cooling. The top part is the measurement part where the in-situ Dynamic Light Scattering probe (Vasco Flex, Cordouan Technology, Pessac, France) is placed and measures directly into the solution (as described in supplemental information, section S1, Fig. S1). The solution was prepared with 5 mg of plastic collected in the North Atlantic in a quartz cell with 50 mL water. Concerning DLS measurement, more details are available in the supplemental information (see section S.1). Each measurement corresponds to five replicates. A control experiment was systematically performed and consisted to hold plastics according to the same experimental conditions without UV irradiation. Finally, the whole experiment was replicated several times. The same tendency than the one described in this paper was observed for each experiment replicate.

Purification and concentration.

Ultrafiltration from the 10kDa to 1.2 µm fraction was conducted using an 8200-Amicon-stirred cell (Milian, Ferney Voltaire, France) with a 10 kDA membrane. Samples were pushed through membranes by using N_2 at a pressure varying from 40 to 100 kPa. Prior to use, all the membranes were washed and left to soak in Milli-Q. Before processing of the sample set, the Amicon cell was abundantly washed with Milli-Q water.

Transmission Electronic Microscopy observation.

Micrographs were taken with LVEM5-TEM (Delong Instrument, Brno, Czech Republic). This instrument is a low-voltage table-sized transmission electron microscope with a Schottky field emission gun. It operates at a nominal acceleration voltage of 5 kV, which is much lower than conventional electron microscope voltages (>90kV). This opens up the possibility of avoiding the heavy metal stains typically used for imaging polymeric and organic molecular materials while preserving a reasonably high resolution (<2 nm). Samples were prepared by directly placing 5 µL of suspension on 300 mesh ultrathin carbon film copper grids (Cu300-HD, Pacific Grid Tech) previously treated by glow discharge using an ELMO system (Cordouan Technologies, Pessac, France) to make the carbon membrane hydrophilic. After removing excess water using a flat filter paper, the TEM grids were air-dried at room temperature for 10 minutes prior to analysis.

Acknowledgements

We thank the Expedition 7ème Continent for the sea sampling campaign and the staff and crew of our expe-

DOI: 10.1039/C6EN00008H

dition: Patrick Deixonne, Frederique Lachot, Marie Bernard, Laurent Morisson, Romain Toutlemonde, and Kris Lemmens. This work is supported by "La mission pour l'interdisciplinarité (MI)" of the French National Center for Scientific Research (CNRS).

References

1 S. Morét-Ferguson, K. L. Law, G. Proskurowski, E. K. Murphy, E. E. Peacock and C. M. Reddy, *Mar. Pollut. Bull.*, 2010, **60**, 1873–1878.

2 V. Hidalgo-Ruz, L. Gutow, R. C. Thompson and M. Thiel, *Environ. Sci. Technol.*, 2012, **46**, 3060–3075.

3 A. A. Koelmans, E. Besseling and W. J. Shim, in *Marine Anthropogenic Litter*, eds. M. Bergmann, L. Gutow and M. Klages, Springer International Publishing, 2015, pp. 325–340.

4 M. Filella, *Environ. Chem.*, 2015, **12**, 527–538.

5 A. L. Andrady, *Mar. Pollut. Bull.*, 2011, **62**, 1596–1605.

6 A. L. Andrady, in *Marine Anthropogenic Litter*, eds. M. Bergmann, L. Gutow and M. Klages, Springer International Publishing, 2015, pp. 57–72.

7 A. Cózar, F. Echevarría, J. I. González-Gordillo, X. Irigoien, B. Úbeda, S. Hernández-León, Á. T. Palma, S. Navarro, J. García-de-Lomas, A. Ruiz, M. L. Fernández-de-Puelles and C. M. Duarte, *Proc. Natl. Acad. Sci.*, 2014, **111**, 10239–10244.

8 L. Van Cauwenberghe, L. Devriese, F. Galgani, J. Robbens and C. R. Janssen, *Mar. Environ. Res.*, 2015, **111**, 5–17.

9 *Exped. 7th Cont.*

10 A. Adelhafidi, I. M. Babaghayou, S. F. Chabira and M. Sebaa, *Procedia - Soc. Behav. Sci.*, 2015, **195**, 2210–2217.

11 L. Douminge, S. Mallarino, S. Cohendoz, X. Feaugas and J. Bernard, *Curr. Appl. Phys.*, 2010, **10**, 1211–1215.

12 M. Gardette, A. Perthue, J.-L. Gardette, T. Janecska, E. Földes, B. Pukánszky and S. Therias, *Polym. Degrad. Stab.*, 2013, **98**, 2383–2390.

13 C. David, M. Trojan, A. Daro and W. Demarteau, *Polym. Degrad. Stab.*, 1992, **37**, 233–245.

14 A. Daro, M. Trojan, R. Jacobs and C. David, *Eur. Polym. J.*, 1990, **26**, 47–52.

15 M. Trojan, A. Daro, R. Jacobs and C. David, *Polym. Degrad. Stab.*, 1990, **28**, 275–287.

16 L. Guadagno, C. Naddeo, V. Vittoria, G. Camino and C. Cagnani, *Polym. Degrad. Stab.*, 2001, **72**, 175–186.

17 M. Liu, A. R. Horrocks and M. E. Hall, *Polym. Degrad. Stab.*, 1995, **49**, 151–161.

18 M. M. El-Awady, *J. Appl. Polym. Sci.*, 2003, **87**, 2365–2371.

19 R. Yang, Y. Li and J. Yu, *Polym. Degrad. Stab.*, 2005, **88**, 168–174.

20 D. Vione, M. Minella, V. Maurino and C. Minero, *Chem. – Eur. J.*, 2014, **20**, 10590–10606.

21 E. Zettler, T. Mincer and L. Amaral-Zettler, *Env. Sci Technol*, 2013, **47**, 7137–7146.

22 J. Lacoste, D. J. Carlsson, S. Falicki and D. M. Wiles, *Polym. Degrad. Stab.*, 1991, **34**, 309–323.

23 A. Tidjani, *Polym. Degrad. Stab.*, 2000, **68**, 465–469.

24 K. N. Fotopoulou and H. K. Karapanagioti, *Mar. Environ. Res.*, 2012, **81**, 70–77.

Electronic Supplementary Material (ESI) for Environmental Science: Nano.

Marine plastic litters: the unanalyzed nano-fraction

Julien Gigault* (1), Boris Pedrono (2), Benoît Maxit (2), Alexandra Ter Halle* (3)

(1) Environnements et Paléo-Environnements Océaniques et Continentaux, French National Center of Scientific Research (CNRS, UMR 5805), 351 Cours de la Libération, 33405 Talence Cedex. *Email: julien.gigault@u-bordeaux.fr
(2) Cordouan Technologies, 11 Avenue de Canteranne, 33600 Pessac
(3) Laboratoire des Interactions Moléculaires et réactivité Chimique et Photochimique (IMRCP), UMR CNRS 5623, Université Paul Sabatier-UPS, Bâtiment 2R1, 3ème étage, 118, route de Narbonne, 31062 Toulouse Cedex 09, France. Email : ter-halle@chimie.ups-tlse.fr

S.1. In-situ Dynamic Light Scattering

Thanks to an optical fiber remote head, the system used in this work is a dedicated DLS system for contact less in-situ measurement as illustrated on Figure S1. The main control unit contains usual blocks for DLS system: Laser, photon counting detector, hardware correlator while an optical fibers umbilical cable acts as an optical link between the main unit and the remote head (it transmits both incident laser towards the head and collected photons towards the detector). The effective probed sample volume could be monitored by switching temporarily a secondary laser trough the scattering optical path. Then the beams crossing point has to be placed within the vial. For the nano-plastics setup, DLS specifications were: laser of 658 nm with a 60mW power; the scattering angle is 170°, the working distance is fixed at 80 mm and the umbilical cable length is 2 m. Those parameters could be modified according to the user constraints.

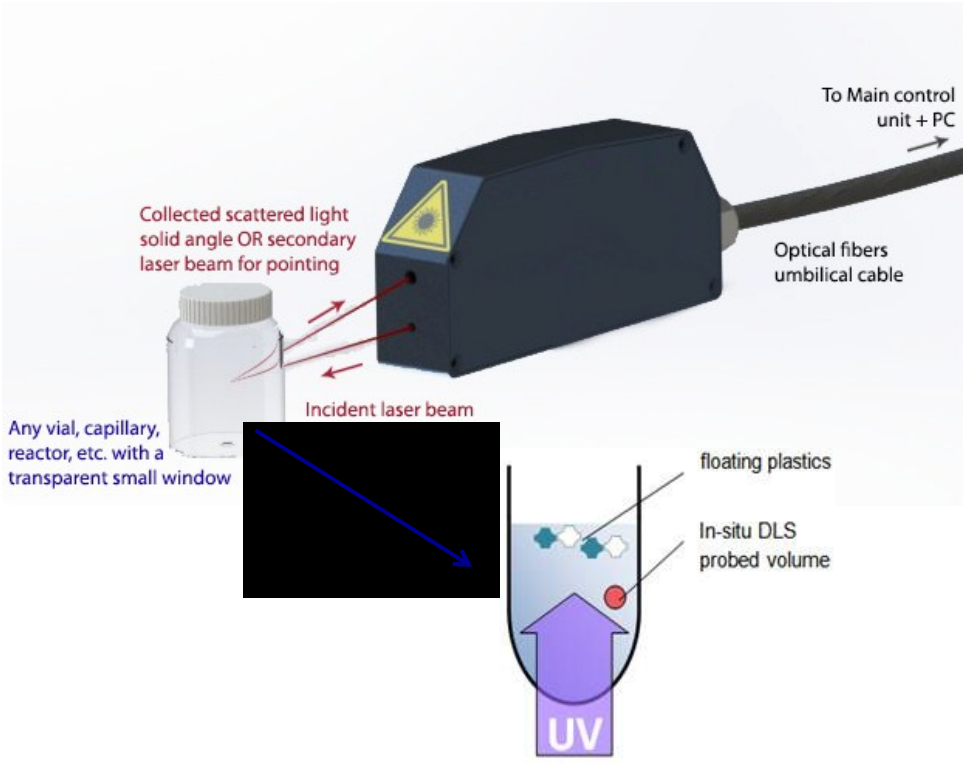

Figure S1: Scheme of the in-situ DLS system coupled to the UV exposition for plastic litters

S.2. Size distribution of nano- and micro-plastics

The figure S2 represents the ACF obtained for highly diluted 200 nm polystyrene (PSL) standards (NIST-traceable Thermo Scientific) (see section S.2) with (red curve) and without (blue curve) additional trace of micro-polystyrene particles standards (few micrometers). The PSL were diluted until the light scattering baselines reached the one obtained for nano- and micro-plastics. The analyses were performed in the same conditions that the ones performed for nano-plastics and micro-plastics evidence.

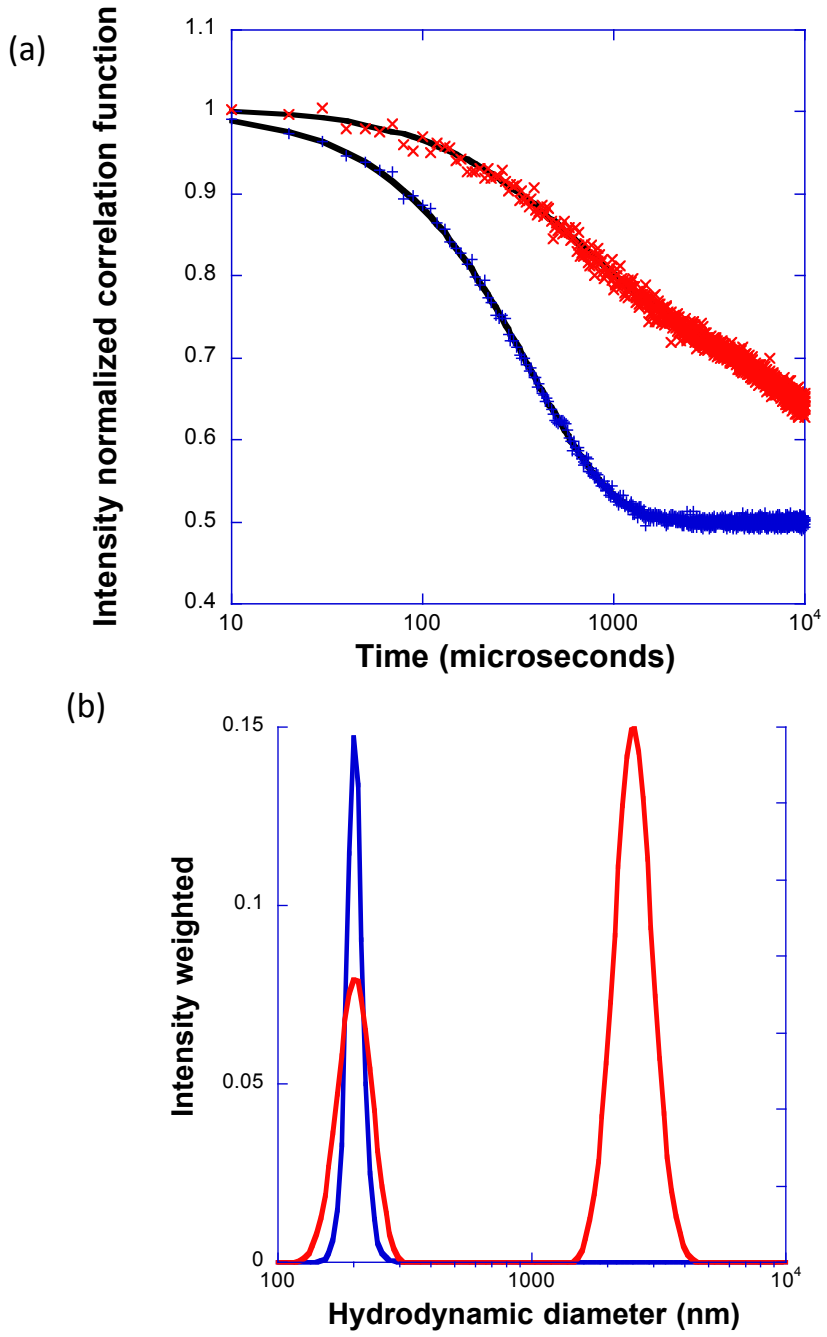

Figure S2: (a) Auto-correlation functions obtained by the in-situ dynamic light scattering detector for highly diluted 200 nm PSL standards in blue and additional trace of micrometer PSL standards in red with the

corresponding fits in black line, with the (b) corresponding Intensity-weighted size distribution size distribution.

S.3. Typical infrared spectra of micro-plastics

Infrared spectra were recorded by attenuated total reflectance (ATR) using diamond ATR crystal on a ThermoNicolet Nexus apparatus. All images were taken with a nominal spectral resolution of 4 cm^{-1}; experiment used 16 scans. The recorded data were corrected in order to obtain transmission-like spectra using ATR Thermo correction (assuming the refractive index of the sample was 1.5).

Microplastics were in polyethylene. Typical methylene absorption band were in the region 1490-1420 cm^{-1} (methylene scissoring peak) and 740-710 cm^{-1} (methylene rocking peak). The oxidation (due to photochemical processes) lead to the formation of carbonyl moieties (carbonyl absorption bands in the region 1760-1690 cm^{-1}). The infrared spectra of the plastic debris were rather complicated compared to PE spectra. Most debris presented an adsorption band at 1540 and 1640 cm^{-1}; it is attributed to amide moieties and could be explained by the presence of the biofilm.

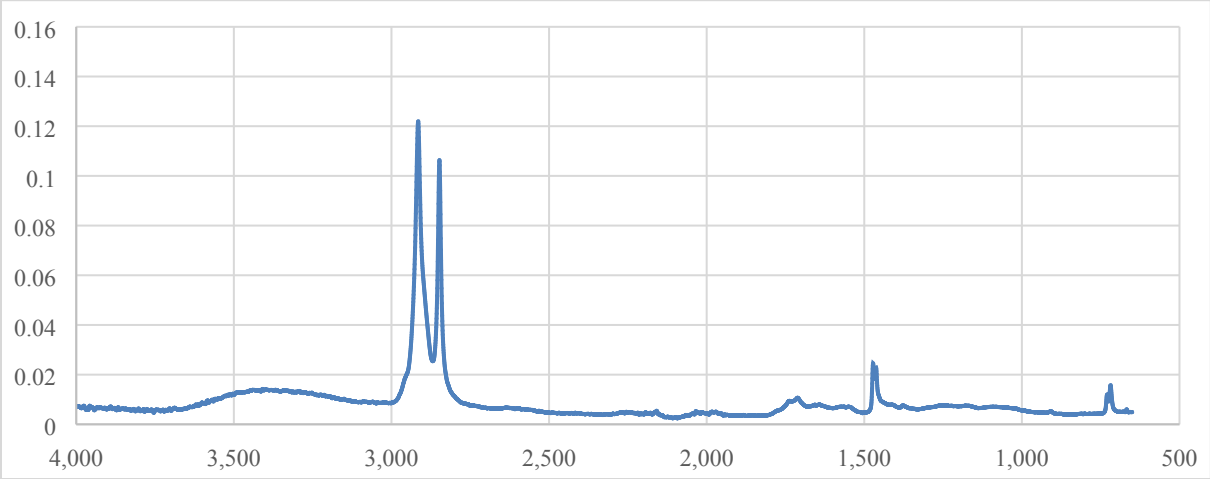

Figure S3: ATR-FTIR spectrum of micro-plastics